Comparison of dynamic properties of ground- and excited-state emission in p-doped InAs/GaAs quantum-dot lasers

Cite as: Appl. Phys. Lett. **104**, 181101 (2014); https://doi.org/10.1063/1.4875238
Submitted: 27 March 2014 • Accepted: 24 April 2014 • Published Online: 07 May 2014

D. Arsenijević, A. Schliwa, H. Schmeckebier, et al.

Comparison of dynamic properties of ground- and excited-state emission in p-doped InAs/GaAs quantum-dot lasers

D. Arsenijević,[1,a)] A. Schliwa,[1] H. Schmeckebier,[1] M. Stubenrauch,[1] M. Spiegelberg,[1] D. Bimberg,[1] V. Mikhelashvili,[2] and G. Eisenstein[1,2]
[1]*Institut für Festkörperphysik, Technische Universität Berlin, Hardenbergstr. 36, 10623 Berlin, Germany*
[2]*Department of Electrical Engineering and The Russell Berrie Nanotechnology Institute, Technion, Haifa 32000, Israel*

(Received 27 March 2014; accepted 24 April 2014; published online 7 May 2014)

The dynamic properties of ground- and excited-state emission in InAs/GaAs quantum-dot lasers operating close to 1.31 μm are studied systematically. Under low bias conditions, such devices emit on the ground state, and switch to emission from the excited state under large drive currents. Modification of one facet reflectivity by deposition of a dichroic mirror yields emission at one of the two quantum-dot states under all bias conditions and enables to properly compare the dynamic properties of lasing from the two different initial states. The larger differential gain of the excited state, which follows from its larger degeneracy, as well as its somewhat smaller nonlinear gain compression results in largely improved modulation capabilities. We demonstrate maximum small-signal bandwidths of 10.51 GHz and 16.25 GHz for the ground and excited state, respectively, and correspondingly, large-signal digital modulation capabilities of 15 Gb/s and 22.5 Gb/s. For the excited state, the maximum error-free bit rate is 25 Gb/s. © *2014 AIP Publishing LLC*.
[http://dx.doi.org/10.1063/1.4875238]

Quantum-dot (QD) lasers have many superior properties mostly traced back to the three dimensional carrier confinement.[1] These include ultra-low,[2] temperature insensitive[3,4] threshold currents, and low relative intensity noise[5] accompanied by a low (current dependent) linewidth enhancement factor.[6,7] The dynamical properties of QD lasers have been modeled[8,9] and studied experimentally using various approaches ranging from complex spectroscopic techniques[10] to direct modulation measurements.[11] A modulation bandwidth of 12 GHz is reported by Kim *et al.* for a 1.28 μm InAs QD laser grown by metal organic chemical vapor deposition.[12] Tunnel-injection structures have been used in order to overcome the gain compression[13] at room temperature caused by hot carrier effects yielding an improved small-signal response of 15 GHz.[14] In combination with p-doping such structures exhibit bandwidths of 13.5 GHz and 25 GHz for excited-state lasers at 1.22 μm[15] and ground-state lasers at 1.1 μm,[16] respectively. However, high-bit-rate digital modulation requires in addition to a large cut-off frequency a linear small-signal response within the $\pm$3-dB window of the response and thus, a damped resonance peak is crucial.

The energy level configuration of GaAs-based QD structures comprises at least three distinct confined electronic states termed ground state (GS) and excited states (ES1 and ES2). The GS is twofold degenerate. Piezoelectric interaction and side-plane inequivalence is essential in lifting the degeneracy of the originally six-fold degenerate p-state to a twofold one, as discovered by Stier *et al.*[17] and later experimentally confirmed, e.g., by Heitz *et al.*[18] Ignoring splitting by side-plane inequivalence leads to fourfold degeneracy of one of the then two excited states.[17,19] The intralevel splittings are of much smaller size than the GS vs ES splitting. The fourfold degeneracy of ES1 leads to a larger gain and differential gain as compared to the GS as well as smaller nonlinear gain compression.[18] Consequently, the dynamic properties of ES1 lasers differ considerably from those based on GS emission with larger predicted cut-off frequencies and digital bit rates. The two different states are easily populated and therefore laser emission is observable at GS or ES1 as well as simultaneously from both.[20,21] The dynamical properties of the two emission modes have been addressed by pump-probe measurements of semiconductor optical amplifiers[22] and by direct modulation experiments.[23] However, under normal operation, it is not possible to measure the maximum modulation bandwidth of the GS since this requires large bias levels which naturally saturates the recombination from the GS to the top holes states and, consequently, recombination from the ESs dominates the emission.

This paper reports on comprehensive experimental comparison between the modulation bandwidths of GS and ES1 emission in a 1.3 μm p-doped InAs/GaAs QD laser. Two nominally identical lasers, which under low bias conditions emit at the GS are used. As the bias increases, they exhibit simultaneous GS and ES emission which evolves to ES emission at large currents. One facet reflectivity of each laser was modified by depositing dichroic mirrors, such that one laser emits only at the GS, while in the second laser oscillations are possible only at the ES1. The dynamics of the two different lasers can be examined here under all bias conditions enabling a proper comparison. We demonstrate that the maximum small-signal bandwidth as well as the maximum bit rate of the laser operating in the ES1 is significantly increased compared to the GS emission. The measurements reveal also that the GS responses exhibit a somewhat larger degree of damping as compared to the ES1 response.

[a)]dejan@sol.physik.tu-berlin.de

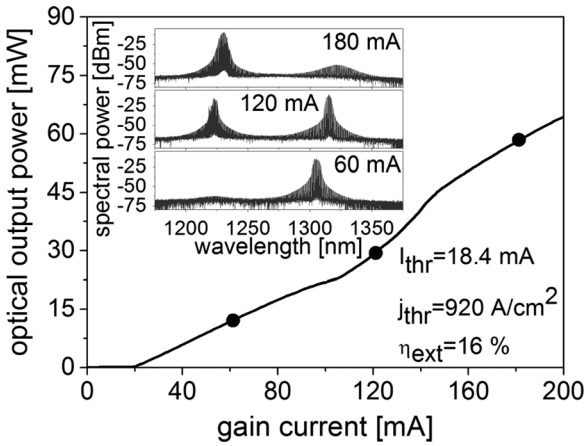

FIG. 1. Continuous-wave power-current characteristics of an uncoated laser at 21 °C. The inset shows corresponding bias dependent optical spectra at 60 mA, 120 mA, and 180 mA.

The devices we have investigated are grown by molecular beam epitaxy on an n+-doped GaAs substrate. The AlGaAs/GaAs laser structure incorporates ten stacked layers of InAs QDs. The GS emission wavelength, close to 1.31 μm, is reached by dot-in-a-well structure (DWELL).[24] In order to achieve low temperature sensitivity of the threshold current[25] and to improve the modulation bandwidth[26] p-doping of 5×10^{17} cm^{-3} in 33 nm GaAs spacers between the QD layers are used. Ridge waveguides with a width of 4 μm and a length of 500 μm were formed by dry etching through the active layer providing strong index guiding of the optical mode as well as suppression of current spreading. Combining Benzocyclobutene-based polymer dielectric interlayers and placing both electrical contacts on the top, minimizes parasitic capacitances resulting in optimized lasers for high-speed operation.[11]

The static characteristics at 21 °C of typical lasers are described in Figure 1 showing ex-facet optical power and optical spectra dependence on bias for the original (uncoated) laser. Two clear thresholds are observed: the first at 18.4 mA (920 A/cm^2) for the GS and the second at 105 mA, where the ES1 turns on. For the linear regime up to 90 mA, the differential external quantum efficiency is 16%. Three representative optical spectra are shown in the inset of Figure 1. At 60 mA, the laser exhibits GS emission at around 1305 nm and a very weak emission at 1225 nm, which represents spontaneous emission at the ES1 energy. For 120 mA, the laser emits simultaneously at both states with essentially the same intensity, while at 180 mA, ES1 dominates and the GS emission intensity is all but diminished.

The rear facet reflectivity of each laser was modified by depositing a specific dichroic mirror with SiO_2 serving as the low index material and Ta_2O_5 for the high index material. Each mirror comprised eighteen layers (nine pairs). In one laser, the dichroic mirror had a reflectivity of 95% at 1305 nm and less than 2% at 1225 nm. This modification reduces the threshold for the GS lasing to 13.8 mA (690 A/cm^2) and completely inhibits oscillation at the ES1 energy. An emission spectrum at 150 mA and the power versus current characteristics (as inset) are shown in Figure 2(a). The laser is driven now at around eleven times the modified threshold current but emission is still exclusively from the GS. Under present chip mounting conditions the linear lasing regime ranges almost up to 150 mA and the corresponding differential external quantum efficiency is 26%. Above 150 mA the slope is reduced due to heating. The second laser is coated with the complimentary dichroic mirror with a reflectivity of 95% at 1225 nm and about 3% at 1305 nm. The optical power versus current for this laser is shown as inset of Figure 2(b). Now, the ES1 threshold is only 37.7 mA (1885 A/cm^2) and initial power rollover is seen only above 200 mA. The increased differential external quantum efficiency of 34% is a result of the larger gain of the ES1. The spectrum at 200 mA is shown in Figure 2(b). The laser operates exclusively at the ES1 wavelength of 1225 nm. The GS emission is more than 55 dB below the dominating laser line in the order of magnitude of the spontaneous emission underground.

The measurements are complemented by 3D eight-band-kp calculations, which include the effect of strain, piezoelectricity, band-coupling, and Coulomb interactions. We assume a truncated pyramidal $In_{0.8}Ga_{0.2}As$ QD, with a base length of 24.3 nm and a height of 5.7 nm, embedded into an $In_{0.2}Ga_{0.8}As$ quantum well. Cryogenic temperature parameters are employed and the resulting excitonic energies are red-shifted by 90 meV according to Varshnis law. As a result, we obtain a GS-transition wavelength of 1315 nm and an ES transition at 1238 nm in agreement with the experiments. Here, for the ES transition, we accounted for p_x- and p_y-type excited electron and hole states including a small piezoelectricity induces splitting. P_z-type states are neglected as their energies are far away owing to the much stronger z-confinement. The calculated intensity ratio between the GS and the ES transition is found to be almost exactly 1:2.

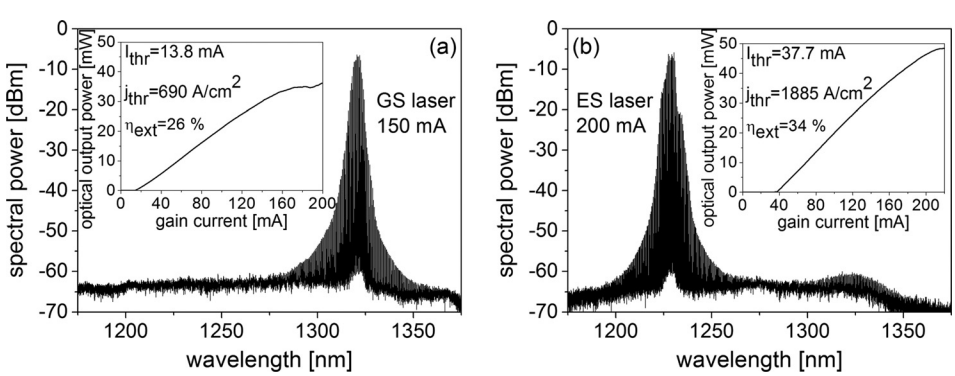

FIG. 2. Optical spectra of the GS (a) and ES1 laser (b) at 150 mA and 200 mA, respectively. The insets show the ex-facet optical power as a function of bias.

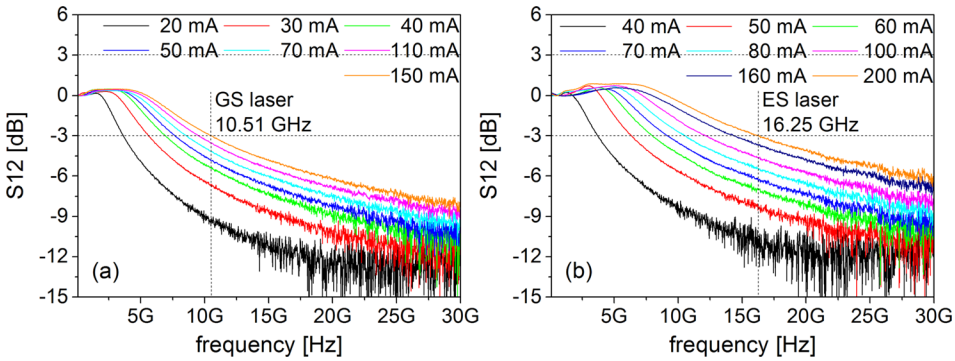

FIG. 3. Small-signal transmission (S_{12}) curves of the two lasers measured at different bias currents: 20–150 mA for the GS (a) and at 40–200 mA for the ES1 laser (b).

The two differently coated lasers are used for modulation measurements in both, the small- and large-signal regimes. For the small-signal measurements, the optical laser signal is coupled to a 50 GHz PIN photodiode. Taking into account the wavelength dependent conversion efficiency and the power dependent photocurrent of the detector, the laser light is attenuated in such a way to provide the same conditions for all measurement points. Figure 3 shows bias dependent small-signal modulation responses for a frequency range of 50 MHz–30 GHz and a modulation amplitude of −10 dBm. The 3-dB-modulation bandwidth is determined directly from the transmission (S_{12}) curves. The GS laser has a maximum bandwidth of 10.51 GHz when driven at 150 mA, which amounts to about eleven times threshold (Figure 3(a)). For currents beyond 150 mA (not shown in the graph), the bandwidth is reduced due to gain saturation and heating, consistent with the corresponding power-current curve shown in Figure 2(a). For the ES1 laser, the maximum bandwidth is 16.25 GHz at a bias of 200 mA, which is around five times threshold (Figure 3(b)). Above 200 mA, the bandwidth does not increase. Also, the responses of the ES1 reveal slightly less gain saturation. This manifests itself in the height of the resonance peak which is 0.4 dB higher for the ES1 laser as compared to the GS laser. Nevertheless, the resonance peak height is always smaller than 0.9 dB, so it does not limit the large-signal response. The enhanced modulation bandwidth of the ES1 represents a record value for any 1.31 μm Fabry-Pérot QD laser; larger than those demonstrated for p-doped tunnel-injection[15] and undoped[23] ES1 lasers.

Large-signal measurements are performed in back-to-back configuration with both lasers. The lasers, which are not matched to 50 Ohm, are directly modulated in the on-off keying (OOK) scheme with a non-return-to-zero (NRZ) pseudo-random binary sequence (PRBS) having a word length of 2^7-1 bits and an amplitude of 0.32 $V_{p\text{-}p}$. The eye diagrams are measured using a 50 GHz photodetector and an 80 GSa/s real-time oscilloscope. The increase in small-signal bandwidth translates of course to the ability to modulate the devices at a higher bit rate in the large-signal regime. Figure 4 compares the large-signal responses of the two states, with the inset of Figure 4(a) showing the eye diagram of the GS laser at a data rate of 15 Gb/s and the maximum received power, where the Q-factor takes on a level of 4.1. For the ES1 laser, the bit rate is 22.5 Gb/s as shown in the inset of Figure 4(b). The corresponding Q-factor is similar, 4.2. Operation of the ES1 laser at 15 Gb/s yields a Q-factor of 7.8 (not shown here). Bit-error ratio (BER) curves are measured at data rates of 15 Gb/s and 22 Gb/s for the GS (Figure 4(a)) and ES1 lasers (Figure 4(b)), respectively. Error-free operation (BER $< 10^{-9}$) is achieved and no error floor is detected. The 3.8 dB power difference at the BER of 10^{-9} mainly results from the difference in bit rate as well as a somewhat larger noise and the lower conversion efficiency of the photodetector at the ES1 wavelength. Thus, the ES1 laser provides a digital bandwidth increased by 7.5 Gb/s as compared to the GS laser.

The maximum error-free bit rate of the ES laser is found to be 25 Gb/s as shown in Figure 5. A clearly open eye is seen with a reduced Q-factor of 3.3. Nevertheless, error-free operation and a BER below 10^{-11} are measured. Compared to the 22.5 Gb/s BER curve the penalty amounts to 0.7 dB at the BER of 10^{-9}. Due to the lower eye height and relatively coarse decision level setting of the error analyzer BER values higher than 10^{-4} cannot be measured accurately.

To conclude, we have demonstrated largely increased modulation bandwidth of ES1 emission derived from the p-states of the QD in p-doped QD lasers as compared to the GS emission. A proper comparison requires that the two modes of operation can be examined under any bias conditions. This is achieved by modification of one laser facet

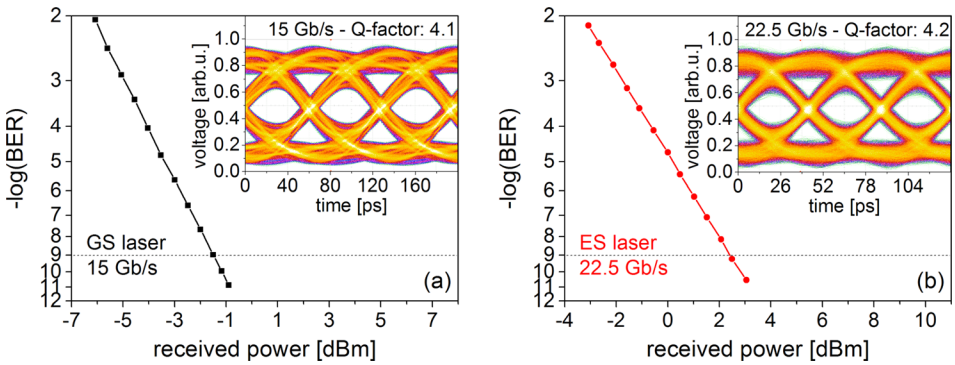

FIG. 4. Bit-error-ratio versus received-power plots and eye diagrams at maximum received power as insets for the GS (a) and ES1 laser (b) at bit rates of 15 Gb/s and 22.5 Gb/s, respectively.

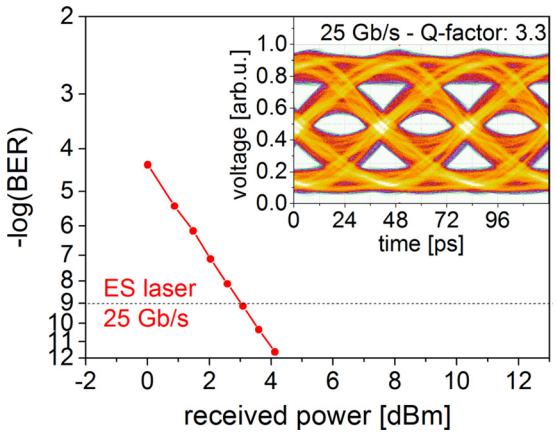

FIG. 5. Bit-error-ratio curve and eye diagram for the ES1 laser driven at the maximum bit rate of 25 Gb/s.

reflectivity by means of a dichroic mirror. Depending on the type of mirror chosen, the laser is shown to oscillate at either the GS or the ES1, but does not switch between the two emission paths. We demonstrate maximum small-signal bandwidths of 10.51 GHz and 16.25 GHz, respectively, and corresponding digital bandwidths of 15 Gb/s and 22.5 Gb/s. For the ES laser, a maximum error-free bit rate of 25 Gb/s is achieved.

The research leading to these results has received funding from the DFG in the framework of the SFB 787 and the Israeli Science Foundation. G. Eisenstein acknowledges support of the Alexander von Humboldt Foundation.

[1]D. Bimberg, N. Kirstaedter, N. N. Ledentsov, Zh. I. Alferov, P. S. Kop'ev, and V. M. Ustinov, IEEE J. Sel. Top. Quantum Electron. **3**, 196 (1997).
[2]R. L. Sellin, Ch. Ribbat, M. Grundmann, N. N. Ledentsov, and D. Bimberg, Appl. Phys. Lett. **78**, 1207 (2001).
[3]O. B. Shchekin and D. G. Deppe, Appl. Phys. Lett. **80**, 3277 (2002).
[4]S. S. Mikhrin, A. R. Kovsh, I. L. Krestnikov, A. V. Kozhukhov, D. A. Livshits, N. N. Ledentsov, Y. M. Shernyakov, I. I. Novikov, M. V. Maximov, V. M. Ustinov, and Zh. I. Alferov, Semicond. Sci. Technol. **20**, 340 (2005).
[5]A. Capua, L. Rozenfeld, V. Mikhelashvili, G. Eisenstein, M. Kuntz, M. Laemmlin, and D. Bimberg, Opt. Express **15**, 5388 (2007).
[6]T. C. Newell, D. J. Bossert, A. Stintz, B. Fuchs, K. J. Malloy, and L. F. Lester, IEEE Photon. Technol. Lett. **11**, 1527 (1999).
[7]J. Kim and S. L. Chuang, IEEE J. Quantum Electron. **42**, 942 (2006).
[8]D. Gready and G. Eisenstein, IEEE J. Sel. Top. Quantum Electron. **19**, 1900307 (2013).
[9]M. Ishida, N. Hatori, T. Akiyama, K. Otsubo, Y. Nakata, H. Ebe, M. Sugawara, and Y. Arakawa, Appl. Phys. Lett. **85**, 4145 (2004).
[10]O. Karni, A. Capua, G. Eisenstein, D. Franke, J. Kreissl, H. Kuenzel, D. Arsenijević, H. Schmeckebier, M. Stubenrauch, M. Kleinert, D. Bimberg, C. Gilfert, and J. P. Reithmaier, Opt. Express **21**, 5715 (2013).
[11]M. Kuntz, G. Fiol, M. Lämmlin, D. Bimberg, M. G. Thompson, K. T. Tan, C. Marinelli, A. Wonfor, R. Sellin, R. V. Penty, I. H. White, V. M. Ustinov, A. E. Zhukov, Yu. M. Shernyakov, A. R. Kovsh, N. N. Ledentsov, C. Schubert, and V. Marembert, New J. Phys. **6**, 181 (2004).
[12]S. M. Kim, Y. Wang, M. Keever, and J. S. Harris, IEEE Photon. Technol. Lett. **16**, 377 (2004).
[13]F. Grillot, B. Dagens, J.-G. Provost, H. Su, and L. F. Lester, IEEE J. Quantum Electron. **44**, 946 (2008).
[14]P. Bhattacharya and S. Ghosh, Appl. Phys. Lett. **80**, 3482 (2002).
[15]C.-S. Lee, P. Bhattacharya, T. Frost, and W. Guo, Appl. Phys. Lett. **98**, 011103 (2011).
[16]S. Fathpour, Z. Mi, and P. Bhattacharya, J. Phys. D: Appl. Phys. **38**, 2103 (2005).
[17]O. Stier, M. Grundmann, and D. Bimberg, Phys. Rev. B **59**, 5688 (1999).
[18]R. Heitz, F. Guffarth, I. Mukhametzhanov, M. Grundmann, A. Madhukar, and D. Bimberg, Phys. Rev. B **62**, 16881 (2000).
[19]A. Schliwa, M. Winkelnkemper, and D. Bimberg, Phys. Rev. B **76**, 205324 (2007).
[20]C. Y. Liu, H. Wang, Q. Meng, B. Gao, and K. S. Ang, Appl. Phys. Express **6**, 102702 (2013).
[21]V. V. Korenev, A. V. Savelyev, A. E. Zhukov, A. V. Omelchenko, and M. V. Maximov, Appl. Phys. Lett. **102**, 112101 (2013).
[22]S. Dommers, V. V. Temnov, U. Woggon, J. Gomis, J. Martinez-Pastor, M. Laemmlin, and D. Bimberg, Appl. Phys. Lett. **90**, 033508 (2007).
[23]B. J. Stevens, D. T. D. Childs, H. Shahid, and R. A. Hogg, Appl. Phys. Lett. **95**, 061101 (2009).
[24]A. R. Kovsh, N. A. Maleev, A. E. Zhukov, S. S. Mikhrin, A. P. Vasilev, E. A. Semenova, Yu. M. Shernyakov, M. V. Maximov, D. A. Livshits, V. M. Ustinov, N. N. Ledentsov, D. Bimberg, and Zh. I. Alferov, J. Cryst. Growth **251**, 729 (2003).
[25]I. P. Marko, N. F. Masse, S. J. Sweeney, A. D. Andreev, A. R. Adams, N. Hatori, and M. Sugawara, Appl. Phys. Lett. **87**, 211114 (2005).
[26]D. G. Deppe, H. Huang, and O. B. Shchekin, IEEE J. Quantum Electron. **38**, 1587 (2002).